ICAS 2021 SHANGHAI
32nd Congress of the International Council of the Aeronautical Sciences
September 6-10, 2021 Pudong Shangri-La, Shanghai, China

BLENDED WING BODY (BWB) PLANFORM MULTIDISCIPLINARY OPTIMISATION (MDO) FOR EARLY STAGE AIRCRAFT DESIGN USING MODEL BASED ENGINEERING

D. Di Pasquale[1], D. Verma[1], G. Pagliuca[1]

1 Centre for Aeronautics, Cranfield University, Cranfield, Bedfordshire, MK430A, UK

Abstract

A model-based engineering (MBE) framework has been developed for Multi-Disciplinary Optimisation (MDO) of a Blended Wing Body (BWB) configuration during early design stages. Specifically, a planform optimisation has been performed by focusing on three objective functions, namely, aerodynamic efficiency (E_{ff}), drag coefficient (C_D) and Operational Empty Weight (OEW). Particle Swarm Optimisation (PSO) has been used as algorithm for the optimisation, an open-source Vortex Lattice Method (VLM), with empirical corrections for compressibility, as aerodynamic module, along with a mass estimation model with respect to BWB considerations. A successful multidisciplinary optimisation has been performed for the BWB-11 configuration flying at cruise condition, specifically at Mach 0.85 and at an altitude of 10 km. Increment in E_{ff} and decrement in C_D and OEW compared to the baseline BWB has been achieved. The OEW has been calculated from a newly developed mass estimation model and successfully validated via statistical methods. The paper presents a rapid MDO framework for efficient BWB planform optimisation to be used at the early design stage, providing useful guidance to the designers. A detailed analysis of the integrated design system, the methods as well as the optimisation results are provided. In addition, further research to the current framework is also presented.

Keywords: MDO, BWB, conceptual aircraft design, PSO, MBE.

1. Introduction

1.1 BWB concept

There has not been any major configurational change in an aircraft since the successful introduction of the Boeing 707 in 1958. Since then the 'Tube and Wing' (TAW) airplane design has dominated the aircraft design. Given the success of the 'tube and wing' aircraft design concept, certain major flaws are yet to be addressed like the increased sound levels and fuel consumption. In the past decades, major aeronautical industries focused their attentions and investments looking at every possible way to improve flight efficiency on commercial airplanes. Nowadays, the key parameter of efficiency has been maximized to the highest level possible, in a point where even slightly improvements will cost millions in terms of investments. ACARE's Flight Path vision for 2050 [1] aims to reduce Carbon-di-Oxide (CO2) and NOx emissions by 75% and 90% respectively per passenger kilometer. Also, perceived noise emissions are expected to decrease by 65%. Flights demanding is exponentially increasing and the aviation industry has the commitment to find a brand-new way of transporting passengers and goods to overcome nowadays problems such as limited fossil fuel reservoirs and alarming global warming levels. Civil aviation faces great challenges because of its robust projected future growth and potential adverse environmental effects. Therefore, it is urgent to limit and to reduce environment impact of aviation by legislation, new infrastructure and flight management, and introduction of new highly effective aircrafts and adoptions of advanced low-emission technologies. During the past decade's investigations, the Blended-Wing-Body (BWB) concept has emerged as a potential solution [2, 3, 4]. The Blended Wing Body is a different approach to commercial aircraft design, utilizing the airframe to produce an efficient lifting surface. The superior aerodynamics of the Blended-Wing Body (BWB) has the potential to reduce the fuel consumption, also by the possibility of having engines that ingest the boundary layer of the centre and reduce noise since the exhaust noise is not reflected by the wing. Therefore, this BWB configuration promises to be a solid candidate for the future commercial aircraft.

1.2 Optimisation overview

The design of modern complex engineering products requires the product definition to be delivered as quickly as possible, to the required functional specification, at the least cost to enable a successful market introduction. This requires the use of appropriate design methods, which are not necessarily the most rigorous, in terms of physical fidelity, or the state-of-the-art. The need for this data to be available rapidly to allow for many concepts and configurations to be assessed in these trade-off studies allows the costs of the conceptual design stage to be minimized.

For an aircraft industry, in order to be competitive in today's global market, where aggressive weight targets, shortened development time scale and reduced costs are the primary objectives and constraints, a different approach for the design process is necessary to be introduced. Optimisation has become part of the design activity in many disciplines that are not only restricted to engineering. Multidisciplinary optimisation represents the new frontier of aircraft design [5]. The motivation behind this inclusion is the need to produce economically relevant products with embedded quality. In the industrial context, optimisation is usually associated with design and it means to identify the best solutions under certain circumstances. Modern design techniques seek for the best design to perform the desired tasks. Engineering optimisation deals with the optimal design of elements and systems in all engineering fields. The main aim of an optimisation process is to find an optimal geometry that fulfils the minimization of the objective functions. In an optimisation problem values of the variables that lead to an optimal value of the function that is to be optimised are sought. In order to improve something, there must be aspects that can be changed. In design optimisation these are called design variables, and collectively they are grouped in a design vector. Hence, design optimisation is the determination of a set of values for the design variables that minimizes (or maximizes) the objective functions and satisfies requirements. Specifically, wing or planform design is dependent on many factors, which must be considered. Changing a wing design parameter may change the overall design of the wing hence making it an iterative process. Raymer [6] mentions that the developmental cost in a new aircraft is massive as compared to the per-plane cost. Thus, multidisciplinary design will be crucial in bringing down the development cost of a new aircraft configuration such as the BWB, by introducing highly automated process, which can perform iterative wing planform designs.

2. Methodology

The optimisation is performed using software units corresponding to distinct disciplines. Generally, applications found in the academic literature provide only a small number of tools to calculate aerodynamic and structural performance. However, early-stage design in the industrial context requires a framework capable of incorporating existing tools and database of experimental data in order to give complete freedom to the designer.

The multidisciplinary planform optimisation workflow schematically shown in Figure 1 is based on a model-based framework [7], where it is implemented via an object-oriented method. Since the research done is an extension of the wing optimisation work performed by Pagliuca [8], a similar implementation of the framework has been adopted. Interface declares input and output for each of the class of models. In turn, a model belonging to a given class must meet the requirements set by the interface, where communication between models is allowed only via the interface. Each model can utilize one or multiple tools to undertake its task such that reusability of data and multi-fidelity approaches are possible. The optimal configurations are found via a Pareto plot which goes through data post-processing in MATLAB, which generates plots, lift-distribution and BWB planform changes.

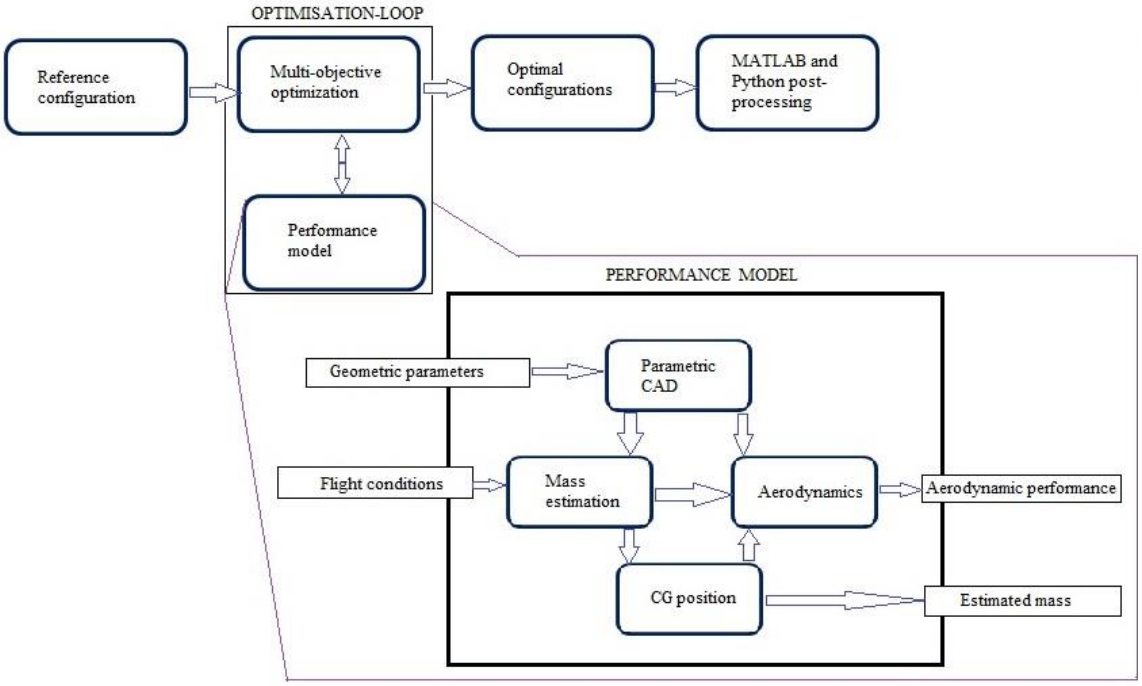

Figure 1 - Optimisation problem workflow.

The optimisation workflow displayed in Figure 1, depicts four blocks for the baseline configuration, an optimiser, a performance model and the optimised configurations. The optimiser interrogates the performance model to compute the objective function and assess new sets of parameters. The optimiser utilized is a single objective PSO algorithm implemented in parallel [9]. It performs a search for global optimality which requires up to thousands of evaluations of the objective functions and searches for optimal configurations using a gradient-free method, which do not rely on differentiable objective functions, and often adopted by engineers to optimise complex systems [10]. They demonstrated to be an efficient choice when a large number of design variables are involved [6], and this is the case of early-design since no ultimate decision about the aircraft configuration is made at that stage. The optimiser takes the weighted sums of all the single objectives. The objective functions considered for objective weighting as previously stated are the aerodynamic efficiency (E_{ff} or L/D), drag coefficient (C_D) and operational empty weight (OEW). Their values are normalized with the performance of the baseline. In this case more weighting is given towards E_{ff}. This approach is similar to the one taken at the conceptual design phase. Certain geometric and stability constrains are adopted to avoid non-sensible configurations. The optimiser interacts with the performance model to produce objective-functions for different optimal configurations, eliminating the configurations that do not lie within the given constraints.

The performance model with the inputs and outputs displayed at the left and right side of the performance model respectively, see bottom part of Figure 1 consists of four models concerning the CAD geometry, mass estimation, aerodynamics and center of gravity (CG) position. The flight conditions and the geometric parameters are input into the performance model by the optimiser. The parametric CAD model is an in-house Cranfield code developed for early-stage design, which produces a new BWB planform geometry. Based on the parametric CAD model, the mass estimation model calculates the aircraft's wing structural mass (e.g. wing ribs etc.) from the methods presented by Howe [11] with the propulsion, nacelle, payload and landing gear calculations done by utilizing equations form Torenbeek [12]. The center of gravity (CG) position is obtained from the mass distribution by a model written on purpose since such information is needed to compute stability derivatives accurately. Then, the aerodynamic takes in the calculated OEW and CG position to trim the aircraft. The design lift-coefficient is calculated by balancing the aircraft's weight.

Regarding the aerodynamic model, the Athena Vortex Lattice (AVL) code [13] is utilized, which operates on a Vortex Lattice Method (VLM) along with the use of empirical methods for transonic corrections. The aerodynamic model takes into account the OEW and CG position value of the aircraft to generate the aerodynamic performance. A Python wrapper is in charge of writing the input files, executing the external tools, and loading the results from output files. Inputs and outputs are performed using files, data is then stored in the performance model. Parallel execution is performed using the multiprocessing module, and results are stored in the Performance model by exploiting inter-process communication. All the models communicate via objected-oriented code written in Python, which facilitates reduction in time, spent transferring data and reusability of the code. The resulting framework is versatile since it incorporates existing tools developed in a variety of programming languages.

2.1 Particle swarm optimisation

According to Coello [14], Particle Swarm Optimisation, is considered an evolutionary algorithm which is a heuristic search technique simulating a swarm to find the optimal solution. It has been initially introduced by Kennedy and Ebhart [15]. In PSO terminology, swarm or particle, which travel through the search space to find the optimal solution by computing their personal best (pbest), interacting with their neighbors (lbest) and having a global best solution (gbest). The position of each particle is updated according to its own best location (pbest) and the best location of its neighbors (lbest).
If $\vec{x}(t)$ denotes the position of a particle p_i at time-step t then its position is changed by adding the calculated velocity at time-step t as follows:

$$\vec{x}_i(t) = \vec{x}_i(t-1) + \vec{v}_i(t) \tag{1}$$

The velocity vector of each particle at time-step t is found by the social behavior of all the swarm with its neighbor and the cognitive behavior with itself by the following scheme:

$$\vec{v}_i(t) = W\vec{v}_i(t-1) + C_1 r_1(\vec{x}_{pbest_i} - \vec{x}_i(t)) + C_2 r_2(\vec{x}_{leader} - \vec{x}_i(t)) \tag{2}$$

Where,
W = weight (or inertia) factor
$C1$ = cognitive learning factor
$C2$ = social learning factor
r_1, r_2 = Constants ϵ [0, 1]; defined by the user

A larger weight factor W in equation 2 facilitates a more global behavior adopted by the swarm. By Coello's [14] explanation, swarm is affected more by a global success of finding the optimal solution than the success of its neighbors. The constants $C1$ and $C2$ in equation 1 are defined as the 'trust' parameters for controlling the swarm's local and social behavior. Higher value of $C1$ means that the particles in the swarm have most trust in themselves and higher $C2$ value means that the particles in swarm have more trust in its neighbors.

2.1.1 Algorithm

The basic algorithm used in PSO is explained by Venter [16] as follows:

- The optimisation begins with selecting a randomly distributed set of particles in the design space (In this research, the randomly set of particles are the planform configurations).
- The velocity vector for each particle is calculated through equation 2.
- The position of each particle is updated by utilizing the velocity calculated in step II through equation 1.
- Steps II and III are repeated until convergence is achieved.

Another explanation is given by Coello [14] is displayed in Figure 2. The optimisation loop begins with the initialization of the swarm particles position and velocity. The corresponding pbest is initialized along with the leader. Then the particle's position and velocity get updated through equations 1 and 2 respectively in each iteration followed by its pbest and the gbest. At the end, the leader is also updated. This continues until convergence is achieved.

```
Begin
    Initialize swarm
    Locate leader
    g = 0
    While g < gmax
            For each particle
                    Update Position (Flight)
                    Evaluation
                    Update pbest
            EndFor
            Update leader
            g++
    EndWhile
End
```

Figure 2 – Pseudocode for general PSO algorithm [14].

2.1.2 Objective weighing

A general optimisation problem consists of several objectives and its associated equality and inequality constraints. The problem is explained as follows:

Minimize/Maximize $f_i(x)$

$$i = 1,2,\dots,N \tag{3}$$

Such that

$$g_j(x) \leq 0 \qquad j = 1,2,\dots,J \tag{4}$$

$$h_k(x) = 0 \qquad k = 1,2,\dots,K \tag{5}$$

where $x = [x_1, x_2, \dots, x_p]$ is a dimensional vector with p decision or design variables and equations 4 and 5 are the inequality and equality constraints.

A common difficulty for multi-objective optimisation problem is the appearance of an objective conflict [17]. Objective conflict as defined by [Hans 1988], occurs when none of the feasible outputs from optimisation give simultaneous optimal solutions for all objectives. Hence mathematically, the most favorable optimal solution in a Pareto will be that solution which provides the least objective conflict [18]. However, such solutions may not satisfy some priorities set by the decision maker [18]. To find such solutions efficiently, scalarization of objective vector into one vector is performed such that all the objective functions find their optimal solutions and certain priorities are met. One such methods of vector scalarization is the method of Objective Weighting.

For this research the method of Objective Weighting is utilized and hence is explained as follows:

$$Z = \Sigma_{i=1}^{N} w_i f_i(x) \tag{6}$$

where $x \in X$, (X is the feasible region)

In equation (6), $f_i(x)$ is the objective vector and weights in weight vector w_i are fractional numbers. The optimal solutions are controlled by the weight vector w_i. Adjusting a corresponding weight in w_i changes the preference of the objective. Mathematically, equal weights for all objectives may generate

least objective conflicts [18]. But priorities should be induced for real world optimisation problems: for this research, aero efficiency (E_{ff}) of the aircraft is given more priority than aircraft's drag (C_D) and weight (OEW) and hence their respective weights are modified accordingly. Usually, each objective is first optimised and all objective functions values are computed at each individual optimum solution. A suitable weight is then chosen for each objective based on their importance and equation (6) is utilized to find the desired solution.

2.2 Mass estimation model

The mass estimation model was developed according to the BWB configuration considerations since the original model utilized by Pagliuca [8] was for a Tube and Wing (TAW) aircraft configuration which would have given non-sensible OEW calculations due to its completely different geometry than the BWB. For the OEW calculations, the structural weight was calculated by the equations from Howe [19] with the propulsion, nacelle, payload and landing gear calculations done by utilizing equations from Torenbeek [20].

2.2.1 BWB Idealization

Since the BWB aircraft is essentially like a flying wing without a proper defined fuselage, a new approach for the idealization was adopted for clear explanation of the optimised results. Figure 3 shows the BWB geometry along with the idealization adopted for defining certain parts. The idealization displayed in figure was defined based on the similar idealization adopted by Howe [18]. The kink station is a semi-span location where the cabin ends, and the front and rear spar begins. The nose is the coordinate (0, 0). The outer and inner wing is the section of the BWB geometry inboard and outboard of the kink station. The weight model in the workflow adopted the same parametric idealization as shown for calculation of the baseline structural weight. Moreover, few terms such as kink station, outer wing and inner wings is used for explanation of the results.

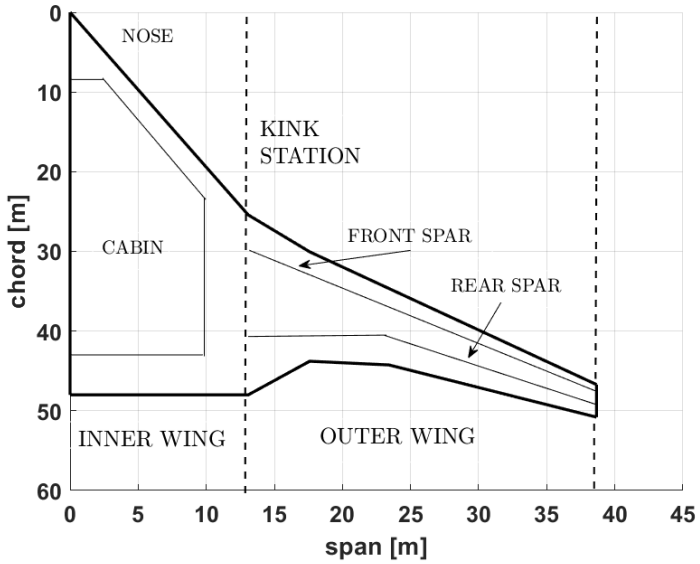

Figure 3 - BWB geometry idealization.

2.2.2 Structural weight calculation

The total structural mass is defined the sum of the inner wing mass, outer wing mass and the 'fuselage section' mass, as presented below:

$$M_{structural} = (M_w)_o + (M_w)_i + (F_i)_f \quad (7)$$

where,

$M_{structural}$ = Total structural mass [kg]

$(M_w)_o$ = Inner wing mass [kg]

$(M_w)_i$ = Outer wing mass [kg]

$(F_i)_f$ = Total 'fuselage' function mass penalty [kg]

The *inner and outer wing mass* was defined by Howe [18] as:

$$(M_w)_X = D_X + (M_r)_X + F_X \tag{8}$$

Where,

D = mass of the wing covers & webs of the structural box [kg]

M_r = mass of wing ribs [kg]

F = penalty function in the outer wing due to the departure from ideal wing box and allowance for secondary structure [kg]

X = subscript notation for outer (o) or inner (i) wing

The *fuselage function mass penalty* defined by Howe [19] is treated by three separate items: Nose fuselage (e.g. – crew accommodation, attachment of nose landing gear unit etc.), main payload mass (e.g.–floor and bulkhead) and secondary structures penalty mass (e.g.–freight doors, emergency exits and windows). Howe [18] mentions that the 'fuselage section' mass uses a theoretical basis and not empirical. That is why, direct values for predicted airframe mass as a percentage of take-off mass (MTOW) for the Cranfield BW-98 aircraft as calculated by Howe [19] is taken (Table 1). From the table, it is clear that:

$$(F_i)_f = (5.48/100) * MTOW \tag{9}$$

Table 1 – Predicted 'fuselage function' mass as a percentage of take-off mass (MTOW) [18]

Component (item)	Mass percentage (%)
Nose fuselage	0.91
Main payload	3.27
Secondary structures	1.3
Total	**5.48**

The full detail on the structural mass of the Blended Wing Body aircraft can be found in Howe [18], and is not presented here for the sake of the length of the paper.

3. BWB optimisation problem formulation

The formulation of the BWB planform optimisation problem is presented in this section. The BWB-11 configuration that has been developed at Cranfield University as research geometry for the assessment of blended wing body aircraft has been taken as the baseline. It was initially derived from the Cranfield Aerospace/BAe Systems Kestrel BWB demonstrator [21] and the Boeing X-48B demonstrator [22]. The three-dimensional (3D) computer aided drawing (CAD) model is displayed in Figure 4 from where parametric dimensions were taken to generate the baseline in the optimisation workflow.

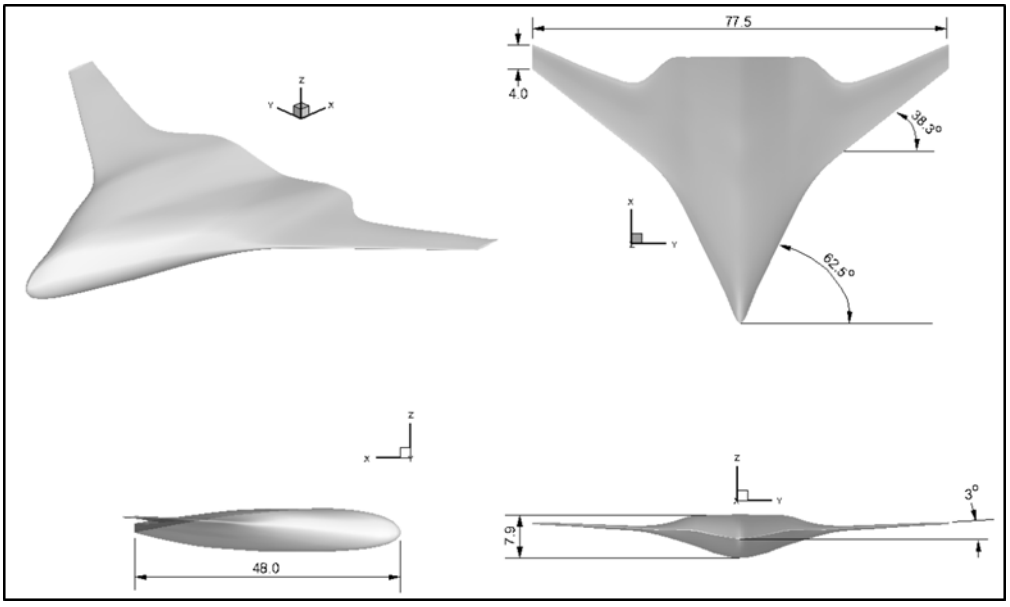

Figure 4 - CAD model of the BWB-11 baseline (units in metres).

The BWB planform has been parametrically defined by twelve geometrical parameters as is shown in Figure 5 (left side). Parameters P1 to P4 and P5 to P8 define the trailing edge and leading-edge location respectively such that the root chord and tip chord length are defined by P1, and P5-P4 respectively. The wing span-wise location is defined by the parameters P9 through P12 along with the representation of the kink station (see Figure 3) chord by P8-P1. Constraints were given to prevent negative sweep angles with M or W-shaped wings and a minimum value was set for the tip chord length of 1.5 meters to avoid pointy wings. Figure 5 (right side) also displays these constraints with C1, C2 and C3, C4 defining the outer wing sweep angles of the trailing and leading edges respectively and C5 denoting the tip chord length. Moreover, the stability derivative was considered to be negative ($dC_m/d\alpha < 1$) such that a longitudinally stable BWB configuration is achieved, where C_m denotes the moment coefficient. Maximum change of the root chord (P1) was constrained to ± 1 meter and all of the other parameters were allowed a maximum change of ± 2 meters.

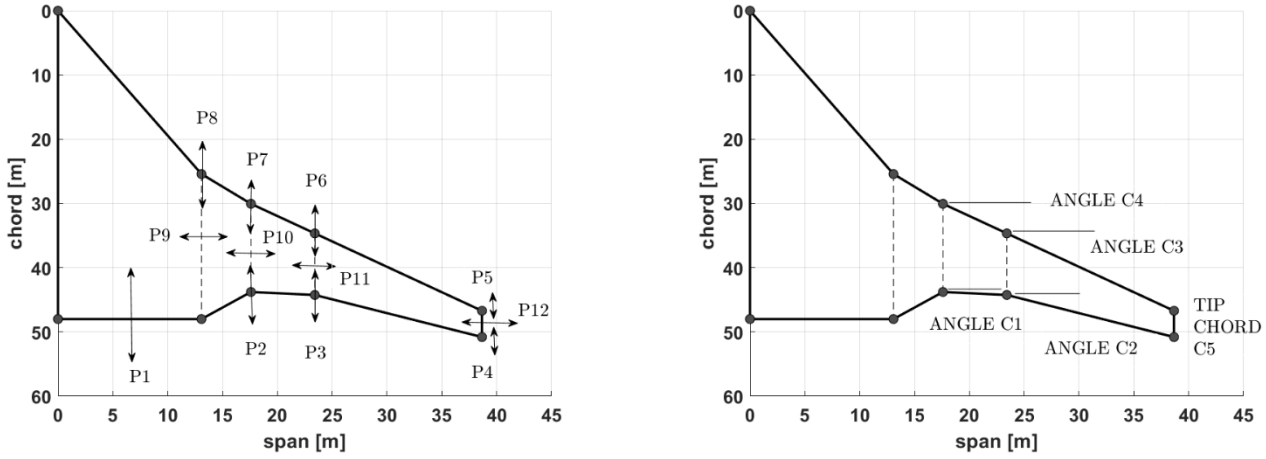

Figure 5 - Geometric parameterisation and constraints.

AVL outputs the angle of attack at which the aircraft is flying based on the given lift-coefficient. A

constraint bracket of (-5, 5) was given for the maximum and minimum angle of attack generated by AVL. Table 2 displays all the mentioned formulation explained above, which has been taken into account for this optimisation problem such that the design targets meet their requirements. The negative sign in front of aerodynamic efficiency (E_{ff}) denotes its maximization in order to reach the design target.

Table 2 – Formulation given to the optimisation problem.

Design target	*minimize: {CD/CD $_{(baseline)}$, OEW/OEW $_{(baseline)}$, -E $_{ff}$/E $_{ff\ (baseline)}$}*
CONSTRAINTS	**CONDITION**
C1, C2, C3 & C4	C3 > C4, C2 > C1
C5	> 1.5 meters
Upper/lower bound (P1)	± 1.0 meter
Upper/lower bound (except P1)	± 2.0 meter

4. Results

A successful optimisation of the BWB planform has been performed for cruise condition flying at M = 0.85 at an Altitude = 10000m and with a baseline OEW = 2.08 x 10^6 kg. The baseline has been defined parametrically based on the planform view of the CAD model shown in Figure 6. The Particle Swarm Optimisation (PSO) algorithm has been used as the optimiser where convergence has been assumed when the maximum distance between swarm particle position and best swarm particle was less than 1 x 10^{-5} at back-to-back iterations. The velocity of the swarm has been updated every iteration by taking 50% of particle's change in position and 50% of the particle's best velocity. The optimiser run with a swarm size of 128 and the maximum number of iterations was set to 10.

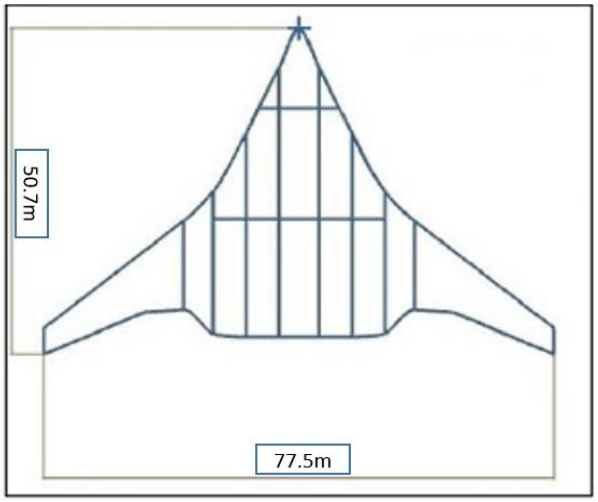

Figure 6: Baseline BWB Planform

VLM along with the empirical corrections for transonic flows have been utilized for the aerodynamic model. The weight model has displayed sensible values for OEW for the baseline and has been successfully validated using a statistical approach based on outliers via Chauvenet's criterion [23] in section 4.4. Three objective-functions are considered for performing optimisations, namely: aerodynamic efficiency (E_{ff}), drag-coefficient (C_D) and OEW. Graph representation is utilized for comparison between the optimised and the baseline planform and their respective lift-distributions. Moreover, the Pareto plot is displayed for double and multi-objective optimisations.

4.1 Single-objective optimisation

Three single-objective optimisations have been performed, specifically maximizing aerodynamic efficiency E_{ff} or L/D, minimizing C_D and minimizing OEW. Please note that E_{ff} and L/D both denote aerodynamic efficiency and the notation E_{ff} will be used hereafter.

Results minimizing/maximizing single-objectives generate impractical values for the objective-functions not being taken into consideration. The objective function being taken into consideration is being maximized/minimized as expected. For example, for E_{ff} maximization there is an increase in E_{ff} by a substantial 4.06%. However, OEW increases by 1.99% even though C_D is decreased by 1.9%. The comparison of the optimised configuration with the baseline is represented in Figure 8. The inner wing stays almost the same as compared to the baseline but the outer wing becomes lightly slender and increases in span, hence the higher lift-distribution, shown in Figure 7 towards the tip chord. For C_D minimization, it has been reduced by 1.61% but an increase in OEW by 0.11% and decrease in E_{ff} by 3.45% has been obtained. This decrease in lift is due to the decrease in total lift in the inner wing as shown in Figure 9. The outer wing is longer with a smaller chord, except near the tip, than the baseline (Figure 10).

There is a decrease in OEW by 1.87% for OEW minimization but C_D increases massively by 10.46% and E_{ff} consequently increases by 2.98%. The total lift is greater just in the inner wing (Figure 11), but the overall configuration is swept back, making the chord smaller throughout the span and the root chord length also decreases, hence decreasing the value of OEW. Single-objective optimisations are generating configurations where the objective function being taken into consideration has been significantly improved, but on the expense of other objective functions. For example, for configuration shown in Figure 11, even though OEW and E_{ff} are meeting the design targets, but there is a massive increase in the drag (10.46%), which is not desirable. Hence, there is a need for a multi-objective consideration.

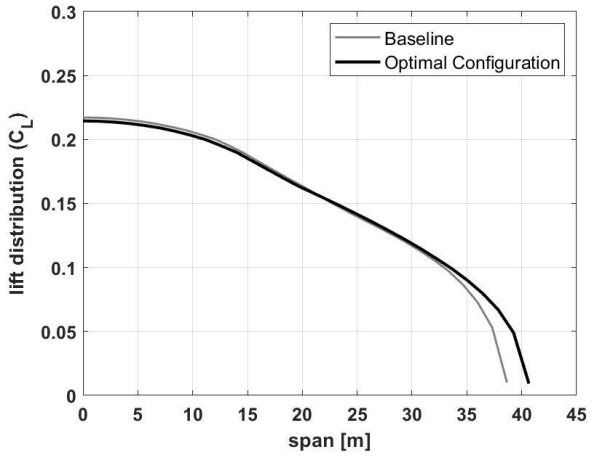

Figure 7 – Lift distribution comparison for maximizing $E_{ff.}$

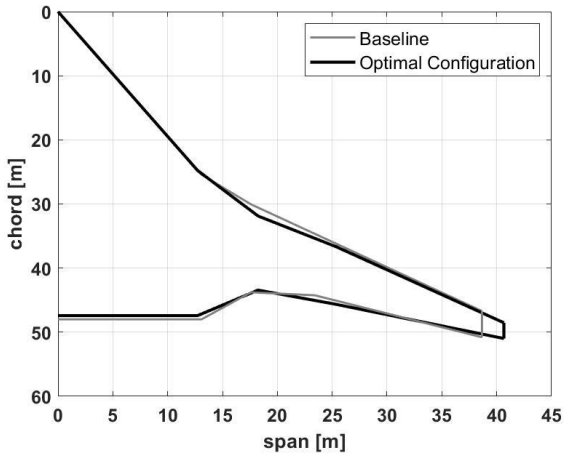

Figure 8 – Planform comparison for maximizing $E_{ff.}$

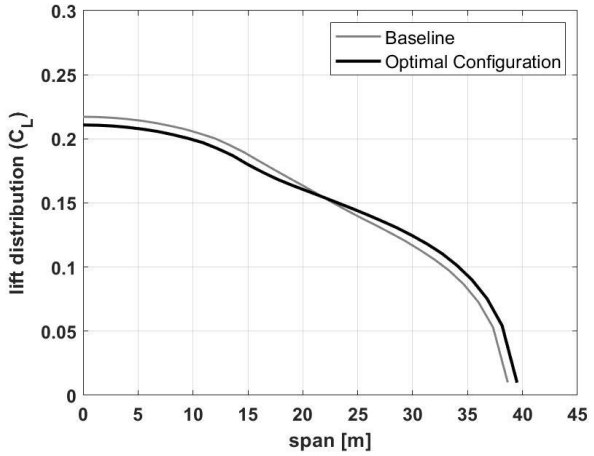

Figure 9 – Lift-distribution comparison for minimizing C_D.

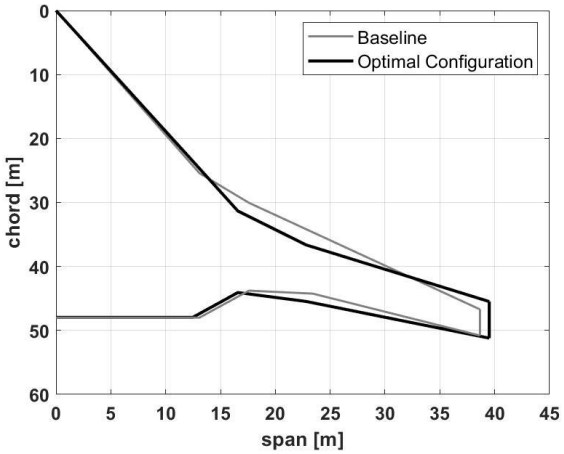

Figure 10 – Planform comparison for minimizing C_D.

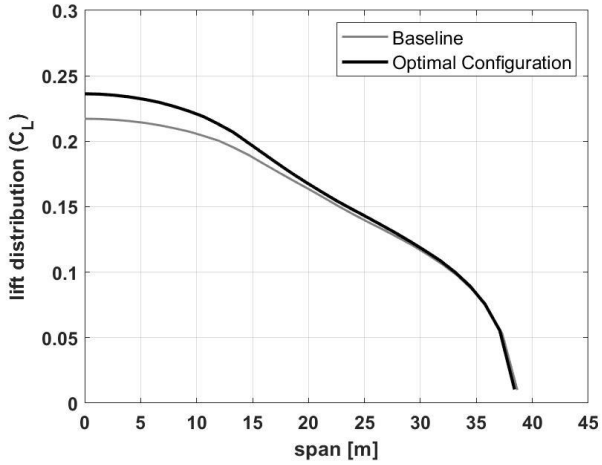

Figure 11 – Lift-distribution comparison for minimizing OEW.

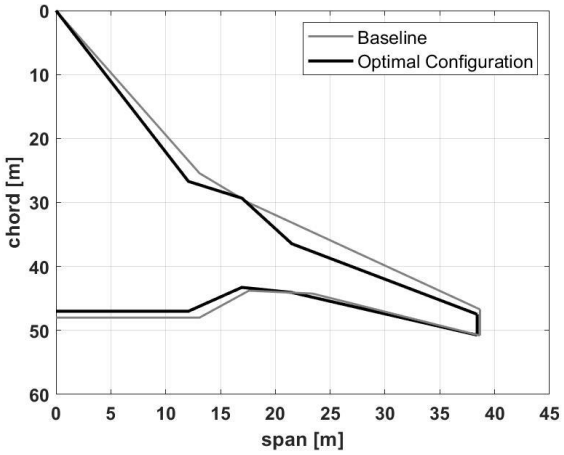

Figure 12 – Planform comparison for minimizing OEW.

4.2 Double-objective optimisation

Thereafter, three double-objective optimisations have been performed: maximizing E_{ff} & minimizing C_D, maximizing E_{ff} & minimizing OEW and minimizing C_D & OEW. The double-objective optimisation generates multiple optimal configurations lying on the pareto front. The authors have chosen a trade-off optimal configuration and the results are presented only for the selected configurations.

Results for the optimisation E_{ff} & C_D are presented first. Figure 13 displays the optimisation result for this particular optimisation. The Pareto front is denoted by black circles, hollow circles denote the optimal configurations which match the design target (i.e. E_{ff} /$E_{ff\ (BWB)}$ >1 and $C_D/C_{D(BWB)}$ < 1). The baseline configuration is displayed by a red cross (i.e. at co-ordinate [1, 1]). Configuration A denoted by solid blue square is the chosen configuration by the authors, which is a trade-off between E_{ff} and C_D values. For this configuration E_{ff} increases by 1.97% and C_D decreases by 3.97% but there is an increase in OEW by 0.36%. The planform and the lift-distribution and comparison of configuration A with the baseline are shown in Figure 14 and Figure 15 respectively. The inner wing remains almost the same with the outer wing becoming gradually thinner. The semi-span length increases by about 2 meters reducing the induced drag. Although the total lift slightly decreases across the wing.

Figure 16 displays the results for E_{ff} and OEW optimisation. The Pareto plot shows that there are five optimal configurations meeting the design target out of which configuration B is the one chosen by the authors. For configuration B, E_{ff} increases by 1.43% and OEW decreases by 1.44% but at the expense of increasing the C_D by 4.75%. The optimal configuration has a greater lift distribution than the baseline (Figure 18). The crank station moves inward and the sweep increases slightly at the inner wing as shown in Figure 17, and the outer wing sweep decreases with a shorter chord length.
Figure 19 shows the optimisation results for the C_D and OEW optimisation where five optimal configurations are generated. Configuration C was chosen as a trade-off configuration by the authors and results comparison for it is presented in Figure 20 and Figure 21. As expected, this optimisation resulted in a decrease in both C_D and OEW by 2.67% and 0.89% respectively; however, there was also a decrease in E_{ff} by 3.25%. The lift-distribution of configuration C is slightly lesser until semi-span length of 20 meters after which it increases and then stays almost the same (Figure 21). As for its planform, the root chord slightly increases, the outer wing significantly changing and the semi-span length decreases slightly. The optimiser successfully improves the two objective-functions being taken into consideration but on the expense of the third one. In all the above configurations, the objective-function not being optimised does not satisfies the design target.

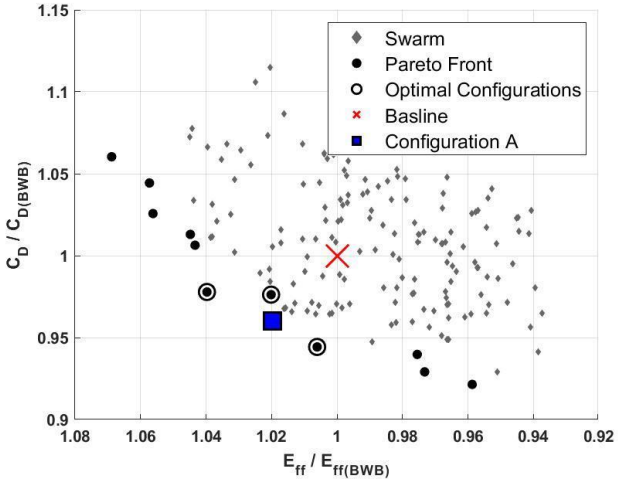

Figure 13 – Pareto plot for E_{ff} and C_D optimisation.

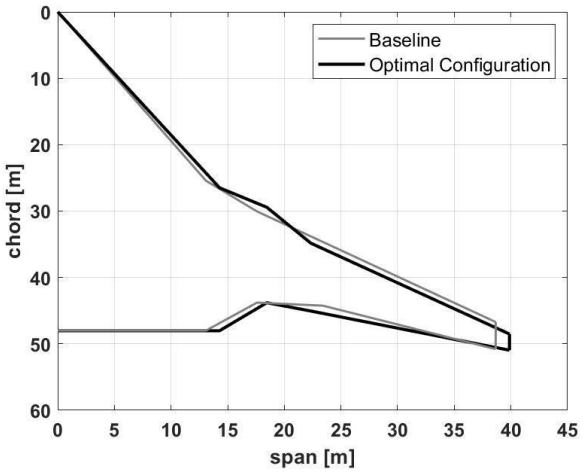

Figure 14 – Planform comparison E_{ff} and C_D optimisation – Configuration A.

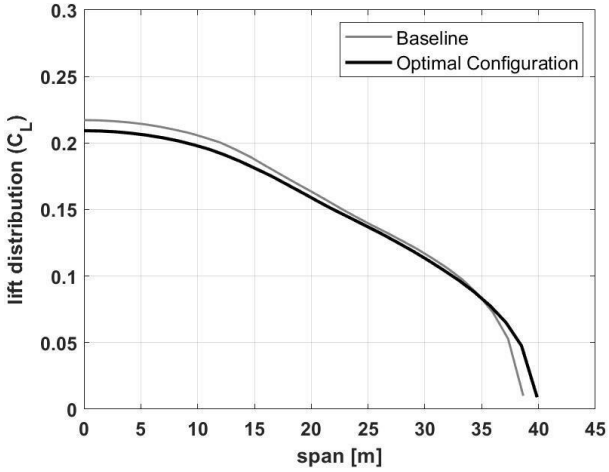

Figure 15 – Lift-distribution comparison E_{ff} and C_D optimisation – Configuration A.

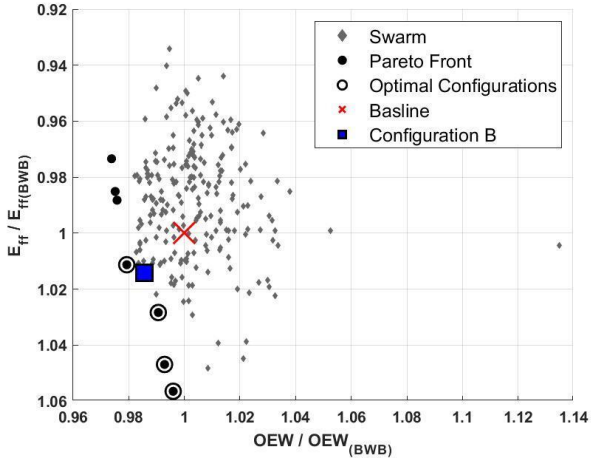

Figure 16 – Pareto plot E_{ff} and OEW optimisation.

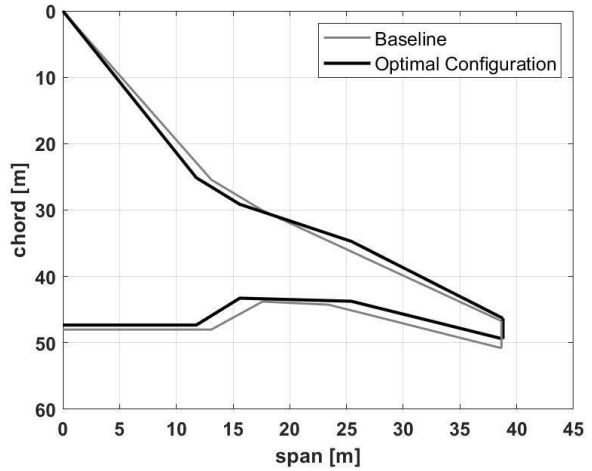

Figure 17 – Planform comparison E_{ff} and OEW optimisation – Configuration B.

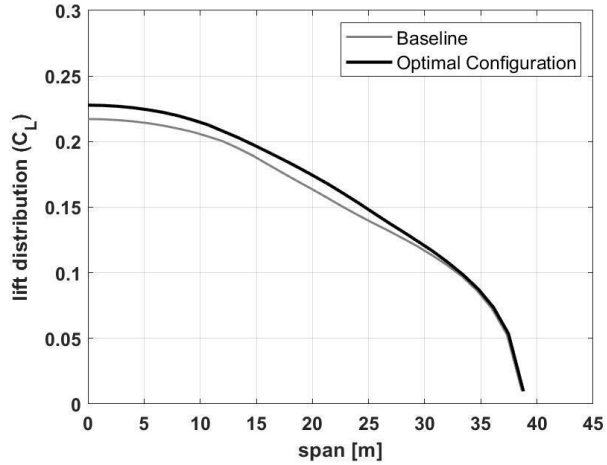

Figure 18 – Lift-distribution comparison E_{ff} and OEW optimisation – Configuration B.

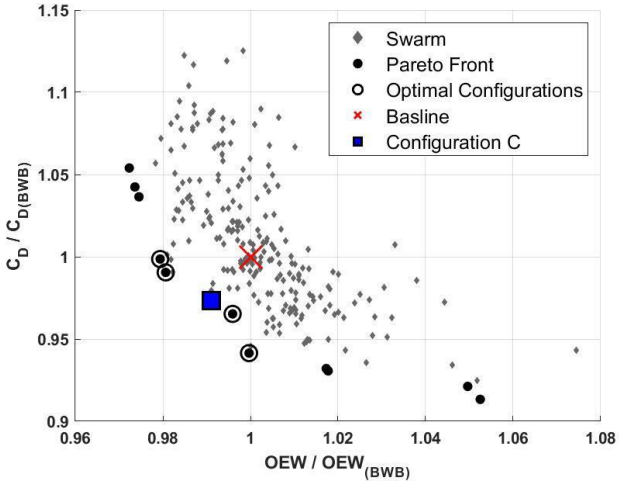

Figure 19 – Pareto plot C_D and OEW optimisation.

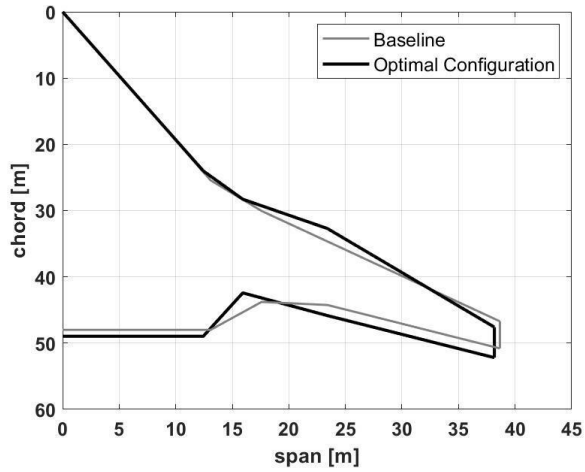

Figure 20 – Planform comparison C_D and OEW optimisation – Configuration C.

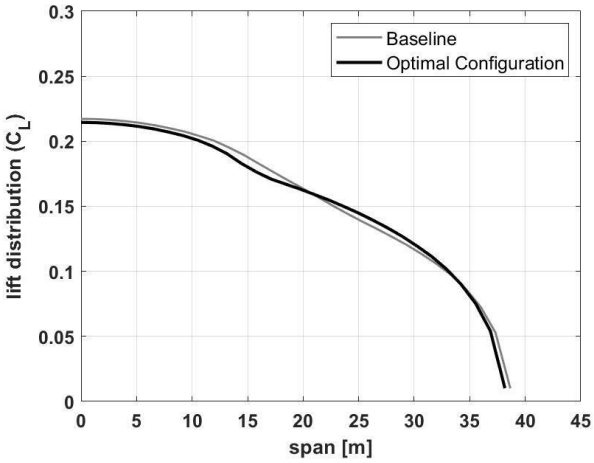

Figure 21 – Lift-distribution comparison C_D and OEW optimisation – Configuration C.

4.3 Triple or multi-objective optimisation

All the three objective-functions being taken into consideration (i.e. E_{ff}, C_D and OEW) have been optimised simultaneously. Since there are three objective-functions, the Pareto (see Figure 22) is a three-dimensional (3D) plot with the C_D, E_{ff} and OEW plotted on the x, y and z-axis respectively. The scale on the E_{ff} axis in Figure 22 is reversed so that the optimal configurations lie towards the bottom-right corner. The notations are identical to the ones in double-objective functions with the baseline is plotted at [1, 1, 1].

The Pareto plot in Figure 22 shows that that there are three optimal configurations which met the design targets (i.e. $E_{ff}/E_{ff(BWB)} > 1$, $C_D / C_{D(BWB)} < 1$ and $OEW / OEW_{BWB} < 1$), out of which configuration D was chosen by the authors. E_{ff} was increased by 2.58% along with the reduction of C_D and OEW by 0.1% and 0.69% respectively.

The lift-distribution of configuration D is compared with the baseline in Figure 24: lift is identical until semi-span length of 17 meters, after which it increases slightly. The inner wing of the optimised configuration D, as displayed in Figure 23, is also identical until the crank station owing to the same lift-distribution, but the outer wing is swept back further with the semi-span length slightly increasing.

The other two optimal configurations in the Pareto plot also produced results where E_{ff} was increasing and C_D, OEW were reducing. Hence, the multi-disciplinary optimisation generates optimal configurations, which meet the design target.

Moreover, the current optimisation algorithm is a single-objective PSO algorithm and replacing it by a double-objective PSO or a genetic algorithm will generate better results. Lastly, the calculation for transonic aerodynamics effects are performed via empirical methods using low-fidelity aerodynamic software (AVL) as the aerodynamic model, which essential assumes the baseline as a two-dimensional flat plate. Inclusion of an aerodynamic analysis via higher-fidelity software such as a Viscous Flow Potential (VFP) code into the aerodynamic model will certainly produce more accurate results as VFP models are able to take into account twist distribution, thickness and formation of transonic shock waves along the wing.

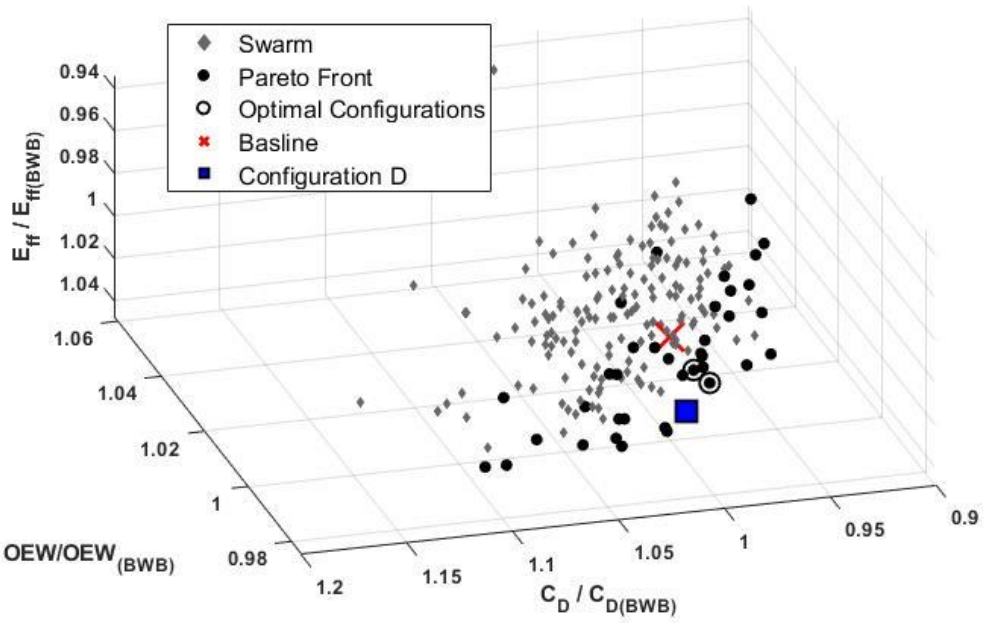

Figure 22 – 3D Pareto plot for multi-disciplinary optimisation.

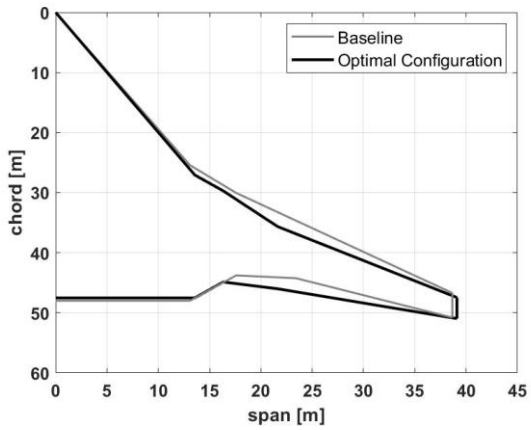

Figure 23 – Planform comparison for multi-disciplinary optimisation.

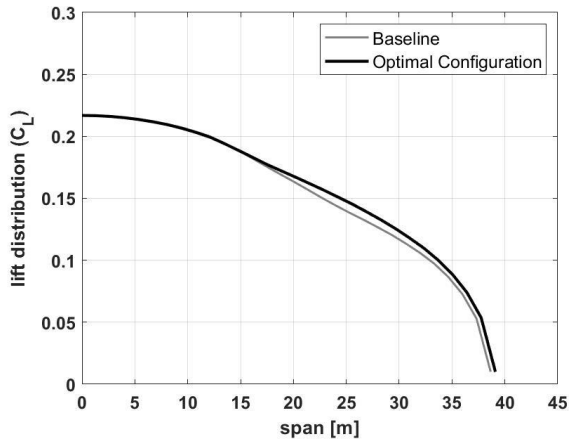

Figure 24 – Lift-distribution comparison for multi-disciplinary optimisation.

4.4 Validation for baseline weight

The weight model in the optimisation workflow has been developed according to the BWB geometry as given in Howe [19]. It can be said that the MDO in the current research takes into account the 'initial sizing' step of the aircraft design in its conceptual phase. Even though Howe [19] has validated his weight calculations but for a slightly different baseline BWB configuration. Moreover, since the research performed is an initial step towards developing a more sophisticated BWB aircraft configuration optimisation, it is important that the OEW calculated is validated. Statistical validation for OEW has been performed via Chauvenet's criterion for outliers' identification [23]. The historical aircraft weight data have been obtained from Roskam [24] and Liebeck's BWB weight data [25] and a linear fit along with the research (baseline) BWB has been performed. Figure 25 shows the linear fir (regression), where Roskam' s data is not shown for clarity and only the line fit and their upper and lower limits are displayed along with another BWB OEW data for consistency. The figure displays that the research BWB lies within the limits.

The location of the research BWB data point in Figure 25 may denote it as an outlier. However, Chauvenet's criterion was successfully applied to all the data points to check if the research BWB is an outlier. Figure 26 shows the plot for the Absolute Z-scores versus the OEW from Roskam, Liebeck and the research BWB-11. It clearly shows that the calculated OEW value for the research BWB model lies below the threshold Chauvenet's Z-score value of 1.960 for the concerned number of data points (10). The exact values for MTOW and OEW for the baseline BWB are marked in Figure 25 as 1,032,645 lb (468,400 kg) and 42,6535 lb (193,473 kg) respectively.

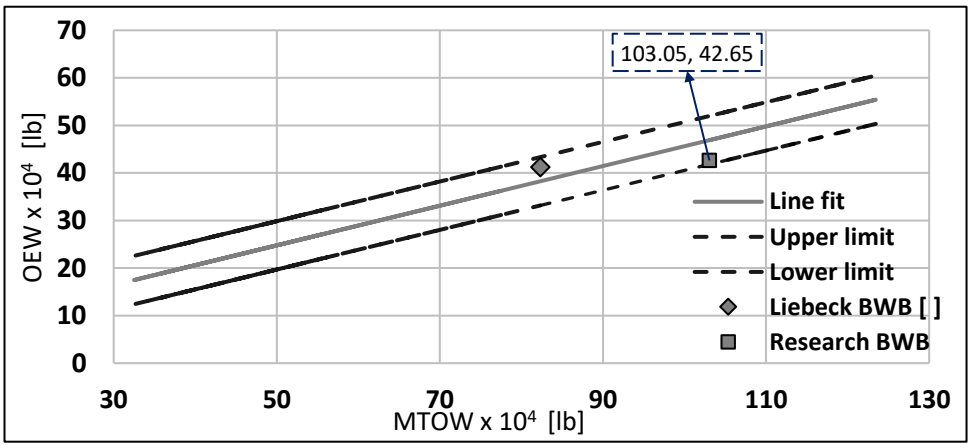

Figure 25 – Linear regression for OEW versus MTOW.

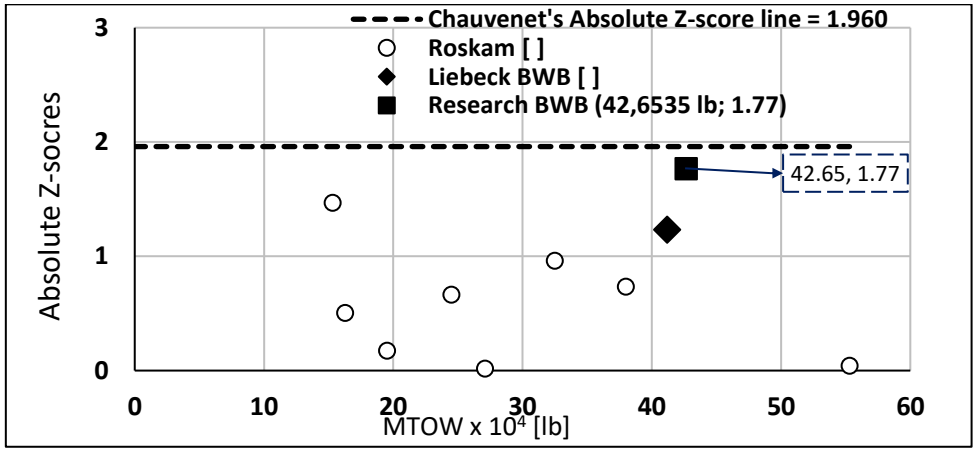

Figure 26 – Chauvenet's criterion check for outliers.

5. Conclusion

A multidisciplinary optimisation was successfully performed on the Blended Wing Body (BWB) aircraft planform flying at Mach 0.85 and 10,000 meters, with the aircraft's maximum take-off weight (MTOW) and the thrust take-off (TTO) taken as 468,400 kilograms and 819,000 Newton respectively. Three objective functions were considered for optimisation namely, aerodynamic efficiency (E_{ff} or L/D), drag coefficient (C_D) and OEW. Maximization of E_{ff} and minimization of C_D and OEW have been considered as design targets. Particle Swarm Optimisation (PSO) has been used as the optimiser algorithm which utilized single objective weighing methods. Open source AVL code [13] along with semi-empirical methods for transonic corrections in drag has been used in the aerodynamics model.

It has been observed that the multi-objective optimisation gave superior aircraft configurations as compared to single and double-objective, which met the design targets in every run. Occasionally, double-objective optimisations may also give configurations which satisfied the design target, but this occurrence was random in nature and it was not assured that the design targets will be met every time. Moreover, multi-disciplinary optimisation (MDO) gave enough optimised configurations which the early stage aircraft designer can choose from for the BWB design. The model-based framework can be used in conceptual design stage for a BWB design to optimize the aircraft at conceptual design phase, which arises a possibility of an already good aircraft design before advancing it to the preliminary design phase. The OEW calculated via developed mass estimation model, which was developed for a BWB configuration was validated successfully through statistical approaches [23].

The BWB aircraft configuration is essentially a flying wing configuration. Hence, any other new and modern wing flying wing designs could potentially utilize this MDO framework at its early design stage due to the short computational time and the reusability that the framework facilitates.

To conclude a useful tool was developed, which is able to take into account targets and constraints coming from multiple disciplines and suggest modifications to the BWB reference geometry.

6. Further research work

The promising MDO research work performed on the BWB configuration is at a preliminary stage where further research is advised by the authors. Furthering this research has the potential to develop the current model-based framework MDO more robust and accurate, which may be utilized by industries or universities for any BWB or flying-wing at early stage design in future. Following are further research, which is advised by the authors and will be performed:

- Optimiser algorithm: The current research utilizes PSO algorithm with an objective weighing method. The optimiser would put more concentration on optimising the single objective on which more stress is given (in this case E_{ff}). Thus, the optimiser will generate configurations with less reduction in OEW and/or C_D. The inclusion of different optimisation algorithms in the framework is advised. For example, Multi-Objective PSO [10, 26] that performs mutation and cross breeding or non-dominated sorting algorithm (NSGA – II proposed by Srinivas and Deb [18]). Both of the mentioned optimisation algorithms does not put weightage on any single objective for optimisation and are the obvious candidates for replacing the current optimiser.
- High fidelity aerodynamic model: A low fidelity open source code AVL is utilized in the aerodynamic model, which essentially considers the BWB planform as a flat surface. Hence, no 3D air-flow effects or any aerofoil transonic aerodynamic characteristics are considered. This might mean that the optimum is a false optimum when considering the sensitivity of viscous and transonic drag more accurately. A higher fidelity Viscous Flow Potential (VFP) [27, 28] method is advised to be included on the framework as it considers the mentioned effects and is more accurate than its counterpart. In fact VFP method was already tested on the same configuration and results have been found in good agreement with RANS solutions as published in [29].

7. Contact Author Email Address

mailto: davide.dipasquale@cranfield.ac.uk

8. Copyright Statement

References

[1] ACARE, *Flightpath 2050 Europe's Vision for Aircraft*. Report of the High-Level Group of Aviation Research, European commission, 2011.

[2] Ayuso L., Moreno R., Sant Palma, and Plágaro Pascual L., Aerodynamic study of a blended wing body; Comparison with a conventional transport airplane, *25th Congr. Int. Counc. Aeronaut. Sci.* 2006, vol. 2, pp. 788–795, 2006.

[3] Qin, N., Vavalle, A., Le Moigne, A., Laban, M., Hackett, K., and Weinerfelt, P., Aerodynamic Considerations of Blended Wing Body Aircraft, *Progress in Aerospace Sciences,* Vol. 40, No. 6, 2004, pp. 321{343. doi:10.1016/j.paerosci.2004.08.001.

[4] Kroo I., Innovations in Aeronautics, *42nd AIAA Aerospace Sciences Meeting,* January 2004. doi:0.2514/6.2004-1.

[5] Slotnick J., Khodadoust A., Alonso J., Darmofal, D., Gropp W., Lurie E., and Mavriplis D., CFD vision 2030 study: a path to revolutionary computational aerosciences. *Technical report*, NASA Langley Research Center, 2013.

[6] Raymer D P. *Enhancing Aircraft Conceptual Design Using Multidisciplinary Optimisation.* Doctoral Thesis, Kungliga Tekniska hongskaloan, Institute of flygteknik, 2002.

[7] Estefan J.A., Survey of model-based systems engineering (MBSE) methodologies. *Incose MBSE Focus Group*, 25(8): 1-12, 2007.

[8] Pagliuca G., Kipouros T. and Savill M., Surrogate Modelling for Wing Planform Multidisciplinary, *Hindawi International Journal of Aerospace Engineering,* Volume 2019, Article ID 4327481, 2019.

[9] Optimisation Using Model-Based EngineeringAudet C, Kokkolaras M. Blackbox and derivative-free optimisation: theory, algorithms and applications, *Optimisation and Engineering*, 17(1): 1–2, Mar 2016.

[10] Reyes-Sierra M and Coello C A. Multi-objective particle swarm optimizers: a survey of the state-of-the-art. *International Journal of Computational Intelligence Research*, 2(3):287–308, 2006.

[11] Howe D. The prediction of aircraft wing mass. Proc. Instn Mech. Engrs, Part G, *Journal of Aerospace Engineering*, 210(G3), pp 135-145, 1996.

[12] Torenbeek E. *Synthesis of Subsonic Airplane Design*, Kluwer Academic Publishers, 1982.

[13] Drela M. and Youngren H. AVL-aerodynamic analysis, trim calculation, dynamic stability analysis, aircraft configuration development. Athena Vortex Lattice, pp. 3-26, 2006.

[14] Coello C.A.C, Pulido G.T, Lechuga M.S., Handling multiple objectives with particle swarm optimisation. *IEEE Transactions on Evolutionary Computation.* Volume: 8, Issue: 3, June 2004.

[15] Kennedy J. and Eberhart R. C. Particle Swarm Optimisation. *Proceedings of the 1995 IEEE International Conference on Neural Networks*. Perth, Australia. Pages pp. 1942-1948, 1995.

[16] Venter G, Sobieszczanski-Sobieski J. Particle Swarm Optimisation. *AIAA Journal*, Vol. 41, No. 8, August 2003. doi.org/10.2514/2.2111

[17] Hans A.E, Multicriteria optimization for highly accurate systems. *Multicriteria Optimization in Engineering and Science*, W. Stadler (Ed.) Mathematical concept and methods in science and engineering, Vol. 19 pp 309-352, 1998.

[18] Srinivas N. and Deb K. Multiobjective Optimisation Using Non-dominated Sorting in Genetic Algorithms, *Journal of Evolutionary Computation*, Vol. 2, No. 3, pp 221-248. 1995.

[19] Howe D. Blended wing body airframe mass prediction, *Proceedings of the Institution of Mechanical Engineers*, Part G: Journal of Aerospace Engineering, Vol. 215, 2001, pp. 319-331.

[20] Torenbeek E. *Advanced aircraft design: Conceptual design, technology and optimisation of subsonic civil airplanes.* John Wiley & Sons, 2013.

[21] Fielding, J.P. & Smith, S. FLAVIIR. An Innovative University/Industry Research Program for Collaborative Research and Demonstration of UAV Technologies. ICAS Paper 2006-0278, *25th International Congress of the Aeronautical Sciences* 2016. Hamburg, Germany, September 2006.

[22] Risch, T., Cosentino, G., Regan, D., Kisska, M. & Princen, N. X-48B Flight-Test Progress Overview *AIAA*

Paper 2009-934, *AIAA 47th Aerospace Sciences Meeting*, 5-8 Jan. 2009, Orlando, Florida, USA. doi:10.2514/6.2009-934.

[23] Jones A R. Outing the outliers – Tails of the Unexpected, International Training Symposium, 2016.

[24] Roskam J.: Airplane design, Part I: Preliminary sizing of aircraft. Lawrence, K.S: Roskam Aviation and Engineering Corporation, 1990.

[25] Liebeck, R.H. Design of the Blended Wing Body Subsonic Transport. Journal of Aircraft, Vol. 41, pp. 10–25, January–February 2004.

[26] Moore J. and Chapman R, Application of particle swarm to multiobjective optimisation, Technical report, Department of Computer Science and Software Engineering, Auburn University, 1999.

[27] Full-potential (FP) method for three-dimensional wings and wing-body combinations – inviscid flow. Part I: Principles and results. ESDU 02013, June 2002 (with Amendment A, May 2006).

[28] Viscous full-potential (VFP) method for three-dimensional wings and wing-body combinations. Part 1: Validation of VFP results with experiment and comparisons with other methods. ESDU 13013.

[29] Prince S.A., Di Pasquale D., Garry K., Progress towards a Rapid Method for Conceptual Aerodynamic Design for Transonic Cruise, *AIAA SciTech Conference*, Orlando, Florida 6-10 Jan 2020.